ISSN: 0976-9102 (ONLINE)
DOI: 10.21917/ijivp.2020.0323

MULTI-FOCUS IMAGE FUSION METHOD WITH QSHIFTN-DTCWT AND MODIFIED PCA IN FREQUENCY PARTITION DOMAIN

C. Rama Mohan[1], S. Kiran[2], Vasudeva[3] and A. Ashok Kumar[4]

[1]*Department of Computer Science Engineering, Visvesvaraya Technological University, India*
[2]*Department of Computer Science Engineering, YSR Engineering College of Yogi Vemana University, India*
[3]*Department of Computer Science Engineering, Shri Madhwa Vadiraja Institute of Technology and Management, India*
[4]*Department of Physics, YSR Engineering College of Yogi Vemana University, India*

Abstract

Multi-focus imaging fusion is a technique that puts together a fully focused object from the partly focused regions of several objects from the same scene. For producing a high quality fused image, directional selectivity and invariance characteristics are important. The ringed artifacts, however, were inserted into a fused image because of a lack of invariance and misdirection. A multi-focus image fusion algorithm is proposed to resolve these issues, in conjunction with qshiftN dual-tree complex wavelet transform and modified principal component analysis. First, the source images are translated into the FP domain. It helps in the obtaining of the row frequency components and column frequency components. Then the row-frequency elements and column-frequency elements are combined with a dual tree-complex wavelet qshiftN to transform the origin frames. Dual tree complex wavelet transforms with qshiftN has demonstrated that it provides an effective transformation for multi-resolution imaging fusion with its directional and shift-invariant characteristics. To enlarge the effectiveness of the qshiftN dual-tree complex wavelet transform in frequency partition-based method, the modified principal component analysis (MPCA) algorithm is used. The proposed fusion approach has been tested on a numeral of multi-focus images and compared to various popular methods of imaging fusion. The experimental results indicate that in subjective performance and objective assessment, the proposed fusion approach could deliver better fusion results.

Keywords:

Multi-focus Image Fusion, Multi-resolution Transform, qshiftN Dual Tree Complex Wavelet Transform, Modified Principal Component Analysis, Quality Evaluation Metrics

1. INTRODUCTION

Due to the restricted focus range of optical lenses in CCD systems, the derivation of an image that includes all the necessary focal objects was impossible [1]. The approach is a multi-focus image fusion that combines several objects from a similar scene into a composite image that is more noticeable and detectable [2]. There are several image fusion methods such as spatial and transform domain methods [3]. Transform domain algorithms, specifically multi-resolution algorithms are better because the human visual system manages multi-resolution information by the transform domain method based computation.

Many multi-resolution methods such as Laplacian pyramid [4], Gradient Pyramid [5], Discrete Wavelet Transformation (DWT) [6], Stationary Transform Wavelet (SWT) [7]-[9], Multi-Resolution Singular Value Decomposition (MSVD) [10], Discrete Cosine Harmonic Wavelet Transform (DCHWT) [11], Transform Wavelet Lifting [12-13], and Double Density Discrete Wavelet Transform (DDDWT) [14] and Shearlet Transform [15] are established in literature. The major issue with pyramid based approaches is the lack of selectivity in the spatial orientation, which generally prone to image blocking effect. This pitfall may be avoided by using DWT however this transformation is confused by the lack of shifting invariance and directionality.

Invariance of changes and directionality are the key elements of the object quality of the fused image. The classical fusion algorithms based on wavelets introduce the ringing artifacts in fused images that limit the utilization of DWT for image fusion. The dual-tree complex wavelet transform (DTCWT) [16] is one of the most accurate wavelet transformers that can easily remove the dearth in invariance and directionality caused by DWT. DTCWT, because it is similar to change and has good directional selectivity. In DTCWT, however, the method of filter design is somewhat complex because of its need to meet both bi-orthogonal and phase specifications. The qshiftN-DTCWT [17] is a method for simplifying the production of filters in DTCWT to produce better fusion performance. The qshiftN-DTCWT has proved its ability to control the directional and change invariant properties as an efficient multi-resolution transform for image fusion.

2. FREQUENCY PARTITION (FP)

Frequency is a periodic motion undergone for one cycle after passing through a series of values. Frequency partition refers to the identification of LF and HF in a given set of data. Further, apply frequency function f which divides LF and HF values separately. Low frequency is indicated here by 'LF' and high frequency is indicated by 'HF'.

In the case of a digital image, low-frequency components are perceptually important. Generally, background components are considered as low-frequency values whereas in the case of high-frequency components sharp image edges are identified which represents foreground components of an image. The frequency partitioning is very useful in the identification of periodic texture patterns or the extraction of features of an image. In the case of a matching procedure, high-frequency components are considered to identify texture pattern.

The fusion process is done separately and combined on both row and column images to prevent noise or distortion. With the help of 1D DCT, vector data has been generated with DCT function $Z(x)$. Further, DCT coefficients are identified for the given vector. Two groups are included in the DCT coefficients for low-frequency and high-frequency components. For energy-compaction of DCT coefficients a partitioning component, f is used that separates DCT coefficients both in low-frequency and high frequency.

$$A(p)=\text{DCT}(a(p)),\ p,v = 0,1,2,\ldots,XY\text{-}1 \quad (1)$$

$$AL(v)=A(v),\ v=0,\ 1,\ 2,\ldots,\ XYf\text{-}1 \quad (2)$$

$$A(v)=A(v),\ v=XYf,\ XYf+1,\ldots,XY\text{-}1 \quad (3)$$

Let the images to be fused are $a_1(p,q)$ and $a_2(p,q)$ and the image fusion process is as follows:

$$a_1(p)=c_2dt_1d(a_1(p,q),X,Y) \quad (4)$$

$$a_2(p)=c_2dt_1d(a_2(p,q),X,Y) \quad (5)$$

$$A_1(v)=\mathrm{DCT}(a_1(p)) \quad (6)$$

$$A_2(v)=\mathrm{DCT}(2(p)) \quad (7)$$

Using Eq.(3), the fused coefficients are:

$$AL_f(v)=0.5(AL_1(v)+AL_2(v)),v=0,1,\ldots,XYf\text{-}1 \quad (8)$$

$$AH_f(v)=\begin{cases} AH_1(v) & if\ |AH_1(v)|\geq|AH_2(v)| \\ AH_2(v) & if\ |AH_1(v)|<|AH_2(v)| \end{cases},$$

$$v=XYf,XYf+1,\ldots,XY\text{-}1 \quad (9)$$

$$A_f(v)=[AL_f(v)\ AH_f(v)] \quad (10)$$

$$a_f(p)=\mathrm{idct}(A_f(v)),\ p,v=0,1,2,\ldots,XY\text{-}1 \quad (11)$$

The fused image is: $I_f=c_1dt_2d(A_f(p),X,Y)$ (12)

where the subscript 1 or 2 or *f* indicates 1st or 2nd or fused image respectively.

3. QSHIFTN-DTCWT

A dearth of the invariance in 1-D and direction sensitivity was found at the DWT, which has been sampled intensively. DTCWT is developed to solve these problems, which is roughly shift-invariant, computing efficient and selective. The DTCWT is an advanced wavelet transformation that uses a dual-tree of wavelet filters to generate the real and imagined parts of transformational coefficients. Two separate two-channel FIR filter banks are used to carry out the DTCWT. The output is called the real part for one of the filter banks (Tree A), and for the other, the output is known as the imaginary part (Tree B).

The DTCWT is using two critically sampled filter banks; a d-dimensional object has a 2d redundancy. The Fig.1 displays structural details of the 1-D DTCWT filter bank structure [17].

Because of its shift-invariance, DTCWT-fused images are smooth and continuous, while DWT-fused images contain irregular edges. DTCWT's other great strength is good directional selectivity, because DTCWT produces six sub-bands for both real and imaginary parts in (±15°,±45°,±75°) at each scale, while DWT provides only minimal directions in (0°,45°,90°), improving transition precision and retaining more comprehensive details.

However, the odd/even filter solution in DTCWT has some problems [16] as discussed below:

1. In the sub-sampling structure, there is no strong symmetry
2. Frequency reactions for both trees are somewhat different;
3. Otherwise, the filter sets must be bi-orthogonal instead of orthogonal because they are linear. It shows that energy conservation does not exist between the signals and the domains.

To minimize and solve all of this, a qshiftN-DTCWT is proposed. The structure of the qshiftN-DTCWT filter [17] is shown in Fig.2 where all filters above level 1 are even short. A sample gap above level 1, 1/2 is achieved with 1/4 and 3/4 delayed filters for a test duration (rather than the 0 and 1/2 of our DTCWT original). It can be done by an asymmetric even-length filter and its time-reverse. These can be built to generate an orthonormal perfect wavelet transformation of the reconstruction due to asymmetry. Tree-A filters reverse are Tree-B filters, and analysis filters reverse are reconstruction filters, so all filters come from the same orthonormal collection. In both trees, the same frequency responses are represented. While the separate responses are asymmetric, symmetric about their midpoints are the integrated complex impulse responses.

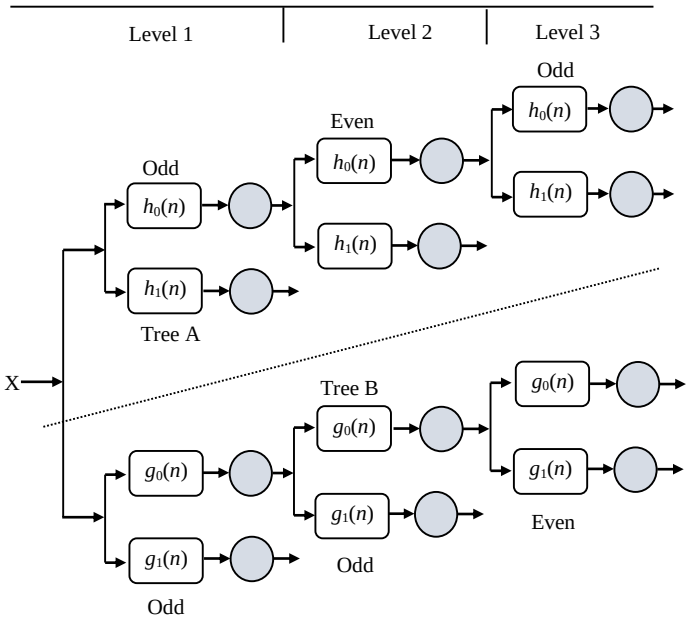

Fig.1. DTCWT Bank Filter Structure

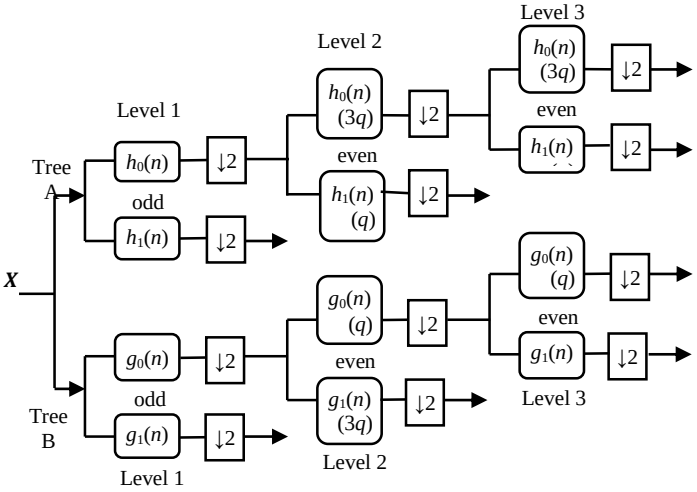

Fig.2. qshiftN-DTCWT filter structure

4. MODIFIED PRINCIPAL COMPONENT ANALYSIS (MPCA)

The MPCA converts associated variables into several non-related main components, as a numerical method. This determines the optimal definition for a particular compact data set. The first principle of MPCA is to estimate covariance values for a given

set of data. The maximum variance is computed from the first principle component.

Let the source image is arranged as one column vector. The following steps are needed to project the data in 1D subspace.

- Arrange the data in a vector.
- Compute the covariance matrix for the given vector.
- Compute Eigenvalues for the given covariance matrix.
- Find out *V, D* from the Eigen function.
- Sort the *D* in order of decreasing eigenvalue.
- The first column computes *V* is the larger value of the Eigen. For estimating *P* as

$$P=V(:,\text{ind}(1))./sum(V(:,ind(1)) \quad (13)$$

- Finally to get the features extracted image as

$$PCA=P(1)*Img \quad (14)$$

To achieve the dimensionality reduction of an image, a novel MPCA method [18]-[20] is formulated, and the MPCA method is explained in Algorithm 1 after image fusion is based on the DTCWT.

Algorithm 1: MPCA method

Input: Fused image by DTCWT.

Step 1: Load the fused image.

Step 2: Compute *C* = *cov*([*im*1(:)])

Step 3: [*V*,*D*] = *eig*(*C*)

Step 4: [*max*,*ind*]=*sort*(*diag*(D), '*descend*')

Step 5: *a* = *V*(:,*ind*(1))./*sum*(*V*(:,*ind*(1)))

Step 6: *F_E_img* = *a*(1)**im*1

Output: Features extracted image.

5. PROPOSED METHOD

The Fig.3 described the flow diagram of the complete fusion algorithm, which consists of two processes such as frequency partition-based qshiftN-DTCWT image fusion process and Modified PCA process.

5.1 QSHIFTN DTCWT BASED IMAGE FUSION IN FREQUENCY PARTITION DOMAIN

The image fusion based on the qshiftN DTCWT based image fusion in Frequency Partition Domain [21]-[23] is described in Algorithm 2, used to apply fusion process to row - frequency and column - frequency components with a partition factor *f*.

Algorithm 2: qshiftN-DTCWT based Image Fusion in Frequency Partition

Input: Multi-focus images.

Step 1. Load the multi-focus images from the source.

Step 2. Perform the frequency partition on multi-focus images to get row and column frequency components.

Step 3. Perform three levels qshiftN-DTCWT on origin image row and column components to generate two low-frequency sub-bands and six high-frequency sub-bands at each level. The following subcomponents are:

$$\left\{\left(L_t^X, H_{l,d}^X\right) \middle| X = A,B;\ l = 1,2,3;\ t = 1,2; d = 1,2,...,6\right\} \quad (15)$$

Step 4. Fuse low- and high-frequency sub-bands using qshiftN DTCWT to obtain composite low- and high-frequency sub-bands.

Step 5. Perform three levels inverse qshiftN-DTCWT on the composited low- and high-frequency sub-bands to obtain the fused image.

Step 6. Apply MPCA on fused image by frequency partition based qshiftN-DTCWT

Step 7. Feature extracted image.

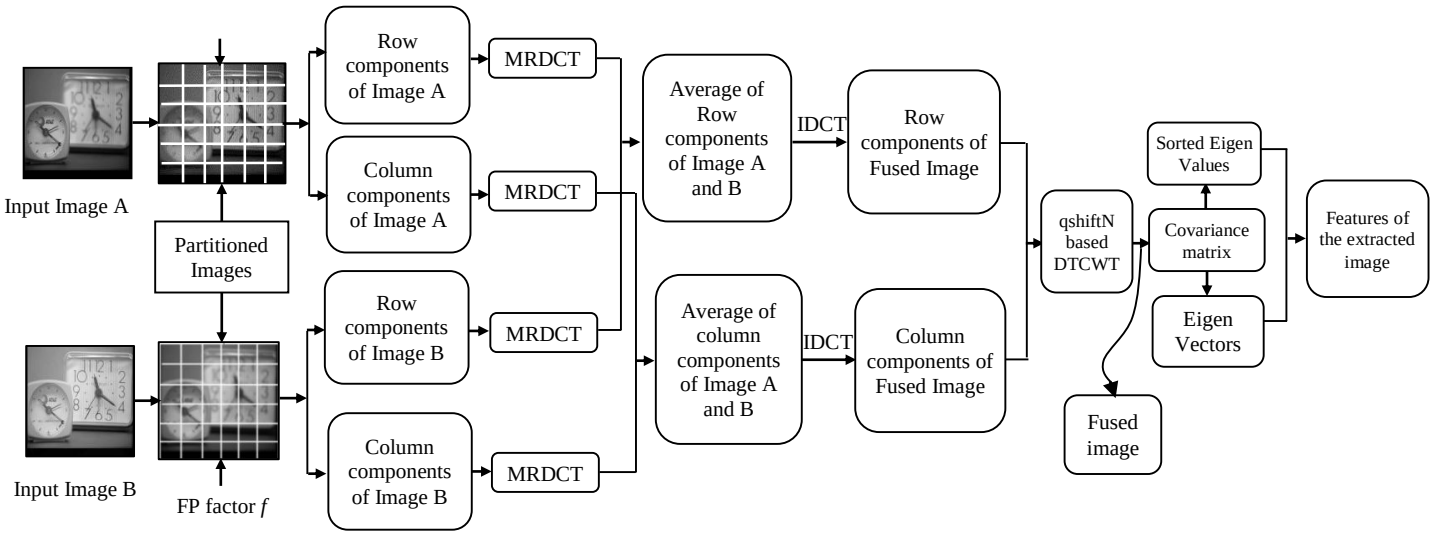

Fig.3. Flow diagram of proposed method

6. RESULTS AND DISCUSSION

Experiments were conducted on different standard multi-focus image test pairs for image fusion research by an online resource (www.mathworks.com). The fusion comparison only applies to five standardized test pairs: multi-focus disk, flowerpot, clock, cameraman and pepsi. The fusion of images by a proposed method (qshiftN-DTCWT and MPCA in FP Domain) is compared with various types of methods: DWT (Discrete Wavelet Transform), MSVD (Multi-resolution Singular Value Decomposition), RP (Ratio Pyramid), LP (Laplacian Pyramid), CVT (Curvelet Transform), SR (Sparse Representation), NSCT (Non-subsampled Contourlet Transform), DTCWT (Dual-tree Complex Wavelet Transform), qshiftN DTCWT-FP, and FP based qshiftN-DTCWT+MPCA. The comparison of performance is based on visual and quantitative measures for performance. All the source images are fused with FP based qshiftN-DTCWT and the dynamic range of an image with MPCA is increased.

Performance measures [24]-[30] such as QS (Piella's Metric), QW (Weighted Fusion Quality), QE1 (Edge-dependent Fusion Quality-Version 1), QE2 (Edge-dependent Fusion Quality-Version 2), QC (Structural Similarity), CQM (Codispersion Fusion Quality), QTE (Tsallis Entropy), QM(Multi-scale Scheme), QP (Phase Congruency), QCB (Chen-Blum Metric), SSIM (Structural Similarity Index Measure), E(F), SD (Standard Deviation), $Q^{AB/F}$ (Edged Based Fusion), AG (Average Gradient), and FMI(Feature Mutual Information) were evaluated for fused images of five sets of multi-focus images. The Table.1 gives the statistical details such as QS, QW, QE1, QE2, QC, CQM, QTE, QM, QP, QCB, SSIM, E(F), SD, $Q^{AB/F}$, AG, and FMI for the multi-focus fused images. If parameters such as QS, QW, QE1, QE2, QC, CQM, QTE, QM, QP, QCB, SSIM, E(F), SD, $Q^{AB/F}$, AG, and FMI are of greater value, the quality of the fused image will be improved. Since the aim of image fusion is to increase the information to make the fused image more appropriate for people's perceptions, visual analysis and quantitative analyses are necessary. In the literature three criterion are frequently used for visual analysis they are (1) transferring information from each picture to a fused image; (2) lost information from the source pictures; and (3) fused artifact.

The fused multi-focus disk images derived through various fusion techniques are illustrated in Fig.4. The Fig.4 shows that, the image quality of the fused disk image (Fig.4(l)) using the proposed method found to be better than other methods without loss of information higher visual quality. It might be necessary, in comparison to other fused images, to merge much of the information from both source images. The statistical parameters in Table.1 can be seen to quantitatively compare the results of the fused multi-focus disk image. The proposed method has demonstrated good performance for all the statistical parameters for a multi-focus disk image.

Visual examination of the flowerpot images fused in Fig.5. Fused imagery can be observed by the proposed method (Fig.5(l)), if compared to other fused images, with a large amount of data from both sources (Fig.5(a) and 5(b)). The Table.1 shows that the performance of the proposed approach in terms of all parameters is superior than compared to other methods. The Fig.6 displays the visual comparison of the fused images by various methods in the multi-focus clock. The fused image quality by the proposed approach (Fig.6(l)) contains more information than the source and has the best visual effects. The Table.1 shows the performance criteria of all test image pairs and the resulting image quality is observed.

The table showed that, about all the statistical parameters, the proposed method is better than other methods expect statistical parameter 'AG'. The fused image of the multi-focus cameraman by different methods is shown in Fig.7. Among the considered fusion methods, the proposed method (Fig.7(l)) has shown with very good image quality in terms of all statistical parameters which was shown in Table.1. In comparison to other algorithms, the statistical parameters achieved by the proposed method yield promising results expect E(F) and SD.

The Fig.8 shows the images of 'pepsi' after different fusion processes using various methods. The fused image derived from the proposed procedure has better visual quality than other fusion-based methods.

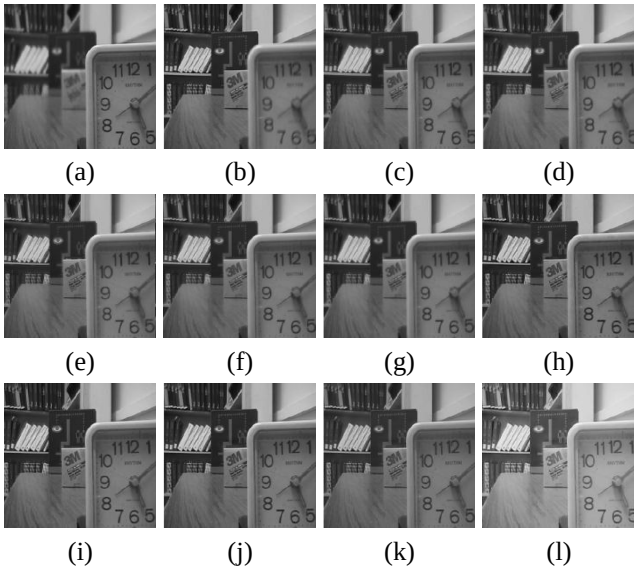

(a) (b) (c) (d)

(e) (f) (g) (h)

(i) (j) (k) (l)

Fig.4. Fusion performance comparison of different fusion approaches (Disk): (a) input image (X), (b) input image (Y), (c) Fused image using DWT, (d) Fused image using MSVD, (e) Fused image using RP, (f) Fused image using LP, (g) Fused image CVT, (h) Fused image using SR, (i) Fused image using NSCT, (j) Fused image using DTCWT, (k) Fused image using DTCWT-FP, (l) Fused image using proposed method

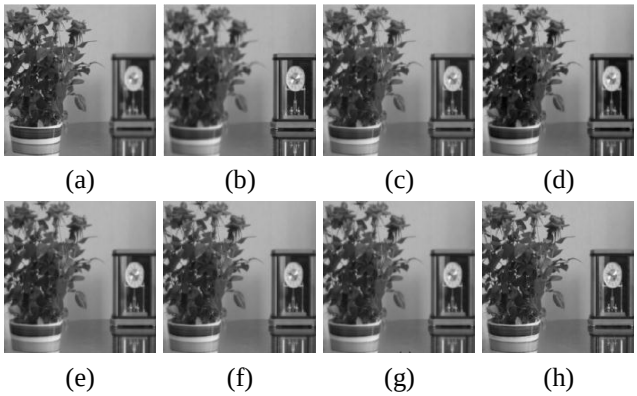

(a) (b) (c) (d)

(e) (f) (g) (h)

(i) (j) (k) (l)

Fig.5. Fusion performance comparison of different fusion approaches (Flowerpot): (a) input image (*X*), (b) input image (*Y*), (c) Fused image using DWT, (d) Fused image using MSVD, (e) Fused image using RP, (f) Fused image using LP, (g) Fused image CVT, (h) Fused image using SR, (i) Fused image using NSCT, (j) Fused image using DTCWT, (k) Fused image using DTCWT-FP, (l) Fused image using Proposed Method

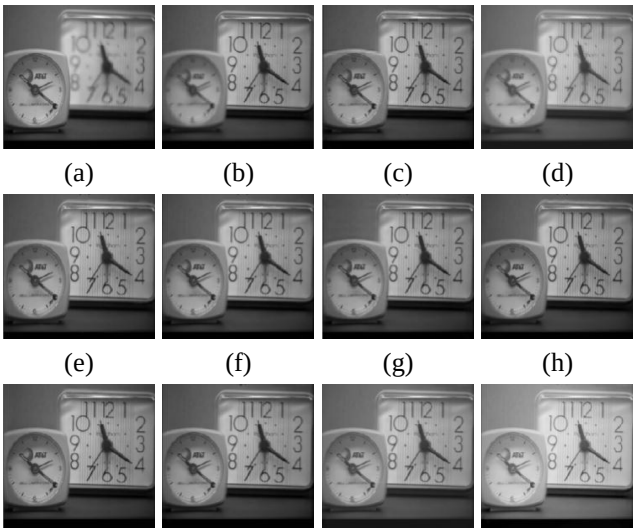

(a) (b) (c) (d)

(e) (f) (g) (h)

(i) (j) (k) (l)

Fig.6. Fusion performance comparison of different fusion approaches (Clock): (a) input image (*X*), (b) input image (*Y*), (c) Fused image using DWT, (d) Fused image using MSVD, (e) Fused image using RP, (f) Fused image using LP, (g) Fused image CVT, (h) Fused image using SR, (i) Fused image using NSCT, (j) Fused image using DTCWT, (k) Fused image using DTCWT-FP, (l) Fused image using proposed method

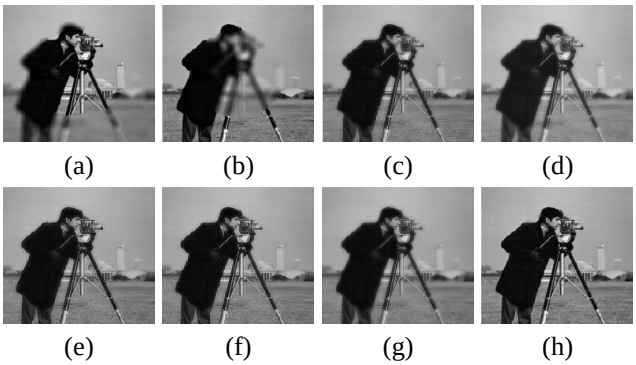

(a) (b) (c) (d)

(e) (f) (g) (h)

(i) (j) (k) (l)

Fig.7. Fusion performance comparison of different fusion approaches (Cameraman): (a) input image (*X*), (b) input image (*Y*), (c) Fused image using DWT, (d) Fused image using MSVD, (e) Fused image using RP, (f) Fused image using LP, (g) Fused image CVT, (h) Fused image using SR, (i) Fused image using NSCT, (j) Fused image using DTCWT, (k) Fused image using DTCWT-FP, (l) Fused image using Proposed Method

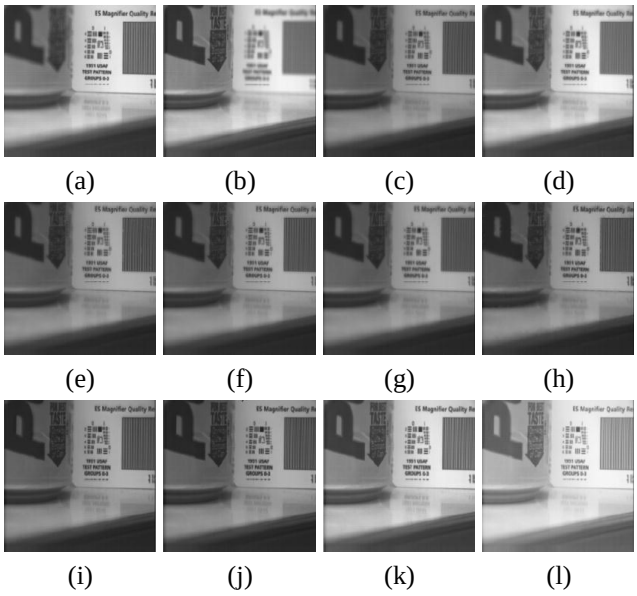

(a) (b) (c) (d)

(e) (f) (g) (h)

(i) (j) (k) (l)

Fig.8. Fusion performance comparison of different fusion approaches (Pepsi): (a) input image (*X*), (b) input image (*Y*), (c) Fused image using DWT, (d) Fused image using MSVD, (e) Fused image using RP, (f) Fused image using LP, (g) Fused image CVT, (h) Fused image using SR, (i) Fused image using NSCT, (j) Fused image using DTCWT, (k) Fused image using DTCWT-FP, (l) Fused image using Proposed Method

The Table.1 shows the statistical parameters of this multi-focus image. The statistical parameters for the proposed method show better numerical values than compared to other techniques.

It is concluded from the results shown in these tables that the proposed algorithm provides better objective results as compared to other algorithms. The statistical results obtained for different multi-focus images has shown that the proposed algorithm shows better performance than compared to other methods published recently elsewhere [17] [29]-[31].

Table.1. Objective evaluation of different fusion methods on the five image pairs with image numbers such as 1. Disk, 2. Flower pot, 3. Clock, 4. Cameraman and 5. Pepsi

Evaluation Metric	Image description	DWT	MSVD	RP	LP	CVT	SR	NSCT	DTCWT	DTCWT-FP	Proposed Method
E(F)	1	7.213667	7.204617	7.249232	7.242373	7.203616	7.308106	7.318048	7.340918	7.33839	**7.352414**
	2	7.365395	7.354879	7.368774	7.372052	7.360904	7.404488	7.410348	7.431975	7.43923	**7.439375**
	3	7.378269	7.277071	7.339356	7.364405	7.39195	7.317128	7.332282	7.342072	7.36999	**7.390612**
	4	7.074522	7.01128	7.055138	**7.077313**	7.068764	7.02295	7.021454	7.047998	7.047953	7.049724
	5	7.101309	7.06786	7.104702	7.102904	7.099343	7.099285	7.104342	7.109221	7.114827	**7.116921**
SD	1	44.50710	44.34168	45.06131	45.11490	44.18472	46.58757	46.88671	46.98573	47.10441	**47.42368**
	2	50.10919	49.56489	50.24224	50.43205	49.95590	52.14527	52.10294	52.55107	52.67039	**52.84863**
	3	51.15215	49.24214	50.84241	51.47436	51.17740	50.71566	51.04213	51.18377	51.24510	**51.32462**
	4	58.54172	57.78185	59.48990	59.65714	58.14892	**62.06411**	61.83622	61.81209	61.85595	61.87614
	5	44.21624	43.65395	44.49203	44.52122	44.01947	44.49950	45.26473	45.40328	45.48391	**45.51261**
$Q^{AB/F}$	1	0.504675	0.491637	0.605551	0.644444	0.496826	0.681104	0.683241	0.686388	0.685828	**0.892203**
	2	0.549380	0.351232	0.592083	0.635865	0.535267	0.670113	0.682003	0.698567	0.699878	**0.807775**
	3	0.69655	0.594634	0.729481	0.744501	0.705347	0.740538	0.737009	0.729067	0.729165	**0.899101**
	4	0.524524	0.399549	0.66256	0.678318	0.521966	0.73679	0.727097	0.728213	0.728122	**0.879017**
	5	0.657477	0.442393	0.72829	0.746194	0.626057	0.714578	0.773076	0.767533	0.76917	**0.859009**
AG	1	6.507383	5.792158	7.450859	7.336186	5.930701	7.821657	8.105431	8.116556	8.117176	**8.131201**
	2	5.623782	3.998212	5.830716	5.818407	5.163203	6.289936	6.481621	6.554996	6.557369	**6.57366**
	3	**9.943426**	8.318444	9.885054	9.862676	9.875922	9.319927	9.660243	9.734923	9.72848	9.646818
	4	12.65051	8.214863	14.05598	13.65031	12.43432	14.16971	14.24701	14.27288	14.27295	**14.28440**
	5	6.715891	4.861793	7.283661	7.296681	6.23593	6.756914	7.800233	7.783991	7.786222	**7.801453**
FMI	1	0.518167	0.487342	0.505812	0.531297	0.47945	0.564561	0.547991	0.556206	0.555509	**0.829334**
	2	0.436781	0.290393	0.477163	0.500922	0.469183	0.515799	0.524388	0.540282	0.542662	**0.710503**
	3	0.589858	0.416048	0.585372	0.599284	0.558481	0.639269	0.593839	0.593908	0.595063	**0.841541**
	4	0.420022	0.36341	0.480561	0.48791	0.41909	0.56126	0.526255	0.536324	0.536138	**0.853631**
	5	0.614670	0.515389	0.644419	0.651092	0.654685	0.669237	0.674566	0.66034	0.660727	**0.815765**
Q_S	1	0.79406	0.787964	0.803947	0.814068	0.792021	0.797382	0.808101	0.776376	0.776799	**0.895112**
	2	0.782448	0.675883	0.786455	0.799849	0.792319	0.755284	0.790282	0.756863	0.757086	**0.850105**
	3	0.830291	0.818294	0.855255	0.851474	0.827152	0.871508	0.84957	0.841501	0.843663	**0.932269**
	4	0.837555	0.675748	0.863412	0.865678	0.831631	0.848779	0.850452	0.833051	0.833189	**0.933972**
	5	0.884735	0.801227	0.89304	0.898024	0.889649	0.896695	0.901765	0.879368	0.879744	**0.945803**
Q_W	1	0.861033	0.857094	0.887154	0.901796	0.851883	0.913005	0.917498	0.910424	0.910402	**0.974451**
	2	0.867793	0.7944	0.881433	0.899807	0.862922	0.913694	0.918159	0.91063	0.910626	**0.939917**
	3	0.924168	0.867759	0.928192	0.929329	0.928115	0.931063	0.93239	0.926104	0.926182	**0.981721**
	4	0.870325	0.827224	0.902473	0.912798	0.863802	0.924128	0.924923	0.92184	0.921855	**0.956007**
	5	0.878899	0.755039	0.922709	0.931639	0.853426	0.915951	0.943879	0.939487	0.939516	**0.951718**
Q_{E1}	1	0.679136	0.645284	0.77517	0.816271	0.623311	0.860081	0.869419	0.863856	0.863819	**0.956879**
	2	0.709974	0.388901	0.754409	0.815015	0.681485	0.873584	0.882238	0.876732	0.876724	**0.91839**
	3	0.82423	0.565512	0.832709	0.843305	0.834944	0.84226	0.84505	0.839886	0.839961	**0.955363**
	4	0.737939	0.595382	0.829645	0.861961	0.699822	0.894296	0.895856	0.89229	0.892302	**0.941126**
	5	0.686957	0.328997	0.838835	0.864726	0.642449	0.804825	0.90583	0.899847	0.899918	**0.922240**
Q_{E2}	1	0.82409	0.80329	0.88043	0.90347	0.7895	0.9274	0.93242	0.92943	0.92941	**0.978200**
	2	0.842599	0.623619	0.868567	0.902781	0.825521	0.934657	0.939275	0.936339	0.936335	**0.958327**
	3	0.907871	0.752005	0.912529	0.918316	0.913752	0.917747	0.91926	0.916453	0.916494	**0.977426**
	4	0.859034	0.77161	0.910848	0.928418	0.836553	0.945672	0.946496	0.944611	0.944617	**0.970116**
	5	0.828828	0.573582	0.915879	0.929906	0.801529	0.89712	0.951751	0.948602	0.94864	**0.960333**

Q_C	1	0.804613	0.797992	0.827856	0.842755	0.800608	0.85668	0.855656	0.851103	0.851021	**0.951077**
	2	0.789626	0.684108	0.800858	0.821806	0.792447	0.807946	0.836364	0.841883	0.841844	**0.914696**
	3	0.835673	0.816826	0.859136	0.859283	0.834006	0.874966	0.8535	0.8548	0.857047	**0.955435**
	4	0.841642	0.689513	0.877764	0.882489	0.832532	0.897312	0.886645	0.883296	0.883537	**0.959561**
	5	0.884217	0.801673	0.893654	0.899258	0.887957	0.901121	0.909411	0.90141	0.902202	**0.954892**
C_{QM}	1	0.895564	0.887944	0.915145	0.923562	0.878508	0.92725	0.933416	0.924928	0.924919	**0.979977**
	2	0.895205	0.844847	0.905442	0.91811	0.885183	0.926882	0.931428	0.922261	0.922253	**0.947197**
	3	0.949537	0.915788	0.951174	0.950475	0.951114	0.952273	0.95421	0.948107	0.948208	**0.988032**
	4	0.903087	0.861325	0.924172	0.930282	0.892105	0.930997	0.934283	0.928735	0.928776	**0.96051**
	5	0.916647	0.826612	0.942709	0.94769	0.874818	0.935275	0.956525	0.953806	0.953827	**0.961314**
Q_{TE}	1	0.363431	0.364408	0.359395	0.356959	0.359396	0.370067	0.36623	0.362058	0.362083	**0.469243**
	2	0.391393	0.365282	0.401482	0.386594	0.389511	0.362928	0.372292	0.370902	0.368748	**0.451988**
	3	0.41905	0.427638	0.424789	0.439668	0.42176	0.431882	0.4279	0.429371	0.429815	**0.488293**
	4	0.427811	0.452554	0.395656	0.420944	0.445997	0.432921	0.444214	0.447297	0.448484	**0.495135**
	5	0.440732	0.423901	0.434663	0.439282	0.446532	0.432071	0.455205	0.441592	0.446906	**0.501893**
Q_M	1	1.362121	0.806232	0.698113	0.811326	0.516705	2.431881	1.842013	2.212968	2.194583	**2.675861**
	2	1.498572	0.510452	0.964673	1.186178	0.917194	2.022972	1.635101	2.015093	2.072246	**2.525475**
	3	2.443449	0.471968	1.897892	2.311507	1.612957	2.072409	1.95843	2.037134	2.035431	**2.663576**
	4	0.976065	0.283111	0.431462	0.58613	0.253984	2.63422	1.937736	2.311687	2.309828	**2.751598**
	5	1.548450	0.704906	1.260219	1.377042	1.040653	1.130443	1.728545	1.836289	1.852415	**2.488504**
Q_P	1	0.598144	0.602709	0.620228	0.716425	0.646076	0.751776	0.755018	0.769584	0.76884	**0.869341**
	2	0.633084	0.414497	0.634209	0.7268	0.663936	0.699196	0.774875	0.801165	0.80125	**0.824598**
	3	0.814985	0.684677	0.849503	0.887645	0.851335	0.874292	0.88975	0.880232	0.881301	**0.952488**
	4	0.66823	0.579439	0.755482	0.800555	0.680163	0.839659	0.839942	0.826334	0.826103	**0.90738**
	5	0.608191	0.447092	0.71085	0.804948	0.748338	0.680215	0.859509	0.840366	0.841147	**0.920652**
Q_{CB}	1	0.517013	0.561885	0.577781	0.569257	0.583337	0.691634	0.659765	0.633933	0.616825	**0.854441**
	2	0.53737	0.525768	0.505774	0.532918	0.531964	0.612368	0.631256	0.702498	0.701229	**0.831178**
	3	0.606661	0.518675	0.746705	0.582521	0.574329	0.750734	0.647031	0.626231	0.623404	**0.877112**
	4	0.388121	0.399906	0.577849	0.530794	0.431007	0.761929	0.672179	0.62591	0.648512	**0.822146**
	5	0.500815	0.50626	0.54574	0.538042	0.483268	0.561986	0.569329	0.673703	0.658537	**0.852505**
SSIM	1	0.941799	0.931191	0.960999	0.971849	0.936346	0.990681	0.989027	0.991612	0.991422	**0.994045**
	2	0.943197	0.893884	0.954100	0.968420	0.943051	0.988164	0.990206	0.992492	0.992450	**0.995323**
	3	0.978569	0.910481	0.986752	0.991081	0.987776	0.990661	0.991718	0.992945	0.992426	**0.997626**
	4	0.939792	0.862835	0.966543	0.973512	0.936271	0.998106	0.993736	0.993300	0.993228	**0.997490**
	5	0.966074	0.927857	0.979171	0.983976	0.962009	0.980845	0.993131	0.991506	0.991443	**0.994474**

7. CONCLUSION

The frequency partition-based qshiftN-DTCWT with MPCA technique was proposed and applied to the image fusion process. Various standard fusion methods have been developed using DWT, MSVD, RP, LP, CVT, SR, NSCT, DTCWT, qshiftN DTCWT-FP and compared with the proposed method. To check the reliability of the images, different quality assurance approaches are evaluated. The proposed Frequency partition-based qshiftN-DTCWT with MPCA shows better performance given assessment metrics, which in turn has better image visual quality without any information loss or objects.

REFERENCES

[1] P. Shah, S.N. Merchant, and U.B. Desai, "Multifocus and Multispectral Image Fusion based on Pixel Significance using Multiresolution Decomposition", *Signal Image and Video Processing*, Vol. 7, No. 1, pp. 95-109, 2013.

[2] Y. Chai, H. Li and Z. Li, "Multifocus Image Fusion Scheme using Focused Region Detection and Multiresolution", *Optics Communications*, Vol. 284, No. 19, pp. 4376-4389, 2011.

[3] B. Zhang, C. Zhang, L. Yuanyuan, W. Jianshuai and L. He, "Multi-Focus Image Fusion Algorithm based on Compound PCNN in Surfacelet Domain", *Optik*, Vol. 125, No. 1, pp. 296-300, 2014.

[4] I.S. Wahyuni and R. Sabre, "Wavelet Decomposition in Laplacian Pyramid for Image Fusion", *International Journal of Signal Processing Systems*, Vol. 4, No. 2, pp. 37-44, 2016.

[5] V. Petrovic and C. Xydeas, "Gradient-based Multiresolution Image Fusion", *IEEE Transactions Image Processing*, Vol. 13, No. 3, pp. 228-237, 2004.

[6] W.W. Wang, P. Shui and G. Song, "Multifocus Image Fusion in Wavelet Domain", *Proceedings of 2nd International Conference on Machine Learning and Cybernetics*, pp. 2887-2890, 2003.

[7] S. Li, B.Yang and J. Hu, "Performance Comparison of Different Multi-Resolution Transforms for Image Fusion", *Information Fusion*, Vol. 12, No. 2, pp. 74-84, 2011.

[8] Abhishek Sharma and Tarun Gulati, "Change Detection from Remotely Sensed Images Based on Stationary Wavelet Transform", *International Journal of Electrical and Computer Engineering*, Vol. 7, No. 6, pp. 3395-3401, 2017.

[9] P. Borwonwatanadelok, W. Rattanapitak and S. Udomhunsakul, "Multi-Focus Image Fusion based on Stationary Wavelet Transform and extended Spatial Frequency Measurement", *Proceedings of International Conference on Electronic Computer Technology*, pp. 77-81, 2009.

[10] V.P.S. Naidu, "Image Fusion Technique using Multi-resolution Singular Value Decomposition", *Defence Science Journal*, Vol. 61, pp. 479-484, 2011.

[11] B.K. Shreyamsha Kumar, "Multifocus and Multispectral Image Fusion based on Pixel Significance using Discrete Cosine Harmonic Wavelet Transform", *Signal, Image and Video Processing*, Vol.7, No. 1, pp.1125-1143, 2013.

[12] H. Li, S. Wei and Y. Chai, "Multifocus Image Fusion Scheme based on Feature Contrast in the Lifting Stationary Wavelet Domain", *EURASIP Journal on Advances in Signal Processing*, Vol. 39, No. 1, pp. 1-16, 2012.

[13] Z. Yuelin, L. Xiaoqiang and T. Wang, "Visible and Infrared Image Fusion using the Lifting Wavelet", *Telecommunication Computing Electronics and Control*, Vol. 11, No. 11, pp. 6290-6295, 2013.

[14] J. Pujar and R.R. Itkarkar, "Image Fusion using Double Density Discrete Wavelet Transform", *International Journal of Computer Science and Network*, Vol. 5, No. 1, pp. 6-10, 2016.

[15] J. Liu, J. Yang and B. Li, "Multi-focus Image Fusion by SML in the Shearlet Subbands", *Indonesian Journal of Electrical Engineering*, Vol. 12, No. 1, pp. 618-626, 2014.

[16] I.W. Selesnick, R.G. Baraniuk and N.G. Kingsbury, "The Dual-Tree Complex Wavelet Transform", *IEEE Signal Processing Magazine*, Vol. 22, No. 2, pp. 123-151, 2005.

[17] N. Radha and T. Ranga Babu, "Performance Evaluation of Quarter Shift Dual Tree Complex Wavelet Transform based Multifocus Image Fusion using Fusion Rules", *International Journal of Electrical and Computer Engineering*, Vol. 9, No. 4, pp. 2377-2385, 2019.

[18] V.P.S. Naidu and J.R. Rao, "Fusion of Out of Focus Images using Principal Component Analysis and Spatial Frequency", *Journal of Aerospace Sciences and Technologies*, Vol. 60, No. 3, pp. 216-225, 2008.

[19] V.P.S. Naidu and J.R. Rao, "Pixel-Level Image Fusion using Wavelets and Principal Component Analysis- Comparative Analysis", *Defence Science Journal*, Vol. 58, No. 3, pp. 338-352, 2008.

[20] S. Wold, K. Esbensen and P. Geladi, "Principal Component Analysis", *Chemometrics and Intelligent Laboratory Systems*, Vol. 2, No. 1-3, pp. 37-52, 1987.

[21] Veerpal Kaur and Jaspreet Kaur, "Frequency Partioning Based Image Fusion for CCTV", *International Journal of Computer Science and Information Technologies*, Vol. 6, No. 4, pp. 3968-3972, 2015.

[22] V.P.S. Naidu, "Novel Image Fusion Techniques using DCT", *International Journal of Computer Science and Business Informatics*, Vol. 5, No. 1, pp. 1-18, 2013.

[23] C.R. Mohan and S. Kiran, "*Image Enrichment using Single Discrete Wavelet Transform Multi-resolution and Frequency Partition*", Artificial Intelligence and Evolutionary Computations in Engineering Systems, Springer, Vol. 668, pp. 87-98, 2018.

[24] P. Jagalingam and A.V. Hegde, "A Review of Quality Metrics for Fused Image, Elsevier Transaction", *Aquatic Procedia*, Vol. 4, No. 1, pp. 133-142, 2015.

[25] Betsy Samuel and N. Vidya, "Full Reference Image Quality Assessment for Biometric Detection", *International Journal of Modern Trends in Engineering and Research*, Vol. 2, No. 6, pp. 453-458, 2015.

[26] M. Gulame, K.R. Joshi and R.S. Kamthe, "A Full Reference Based Objective Image Quality Assessment", *International Journal of Advanced Electrical and Electronics Engineering*, Vol. 2, No. 6, pp. 13-18, 2013.

[27] Ratchakit Sakuldee and Somkait Udomhunsakul, "Objective Performance of Compressed Image Quality Assessments", *Proceedings of World Academy of Science, Engineering and Technology*, Vol. 26, pp. 434-443, 2007.

[28] Kun Zhan, Qiaoqiao Li, Jicai Teng, Mingying Wang and Jinhui Shi, "Multifocus Image Fusion using Phase Congruency", *Electronic Imaging*, Vol. 24, No. 3, pp. 1-12, 2015.

[29] Chinmaya Panigrahy, Ayan Seal and NiharKumar Mahato, "Fractal Dimension based Parameter Adaptive Dual Channel PCNN for Multi-Focus Image Fusion", *Optics and Lasers in Engineering*, Vol. 133, No. 1, pp. 106141-106163, 2020.

[30] Lin He, Xiaomin Yang, Lu Lu, WeiWu, Awais Ahmad and Gwanggil Jeon, "A Novel Multi-Focus Image Fusion Method for Improving Imaging Systems by using Cascade-Forest Model", *EURASIP Journal on Image and Video Processing*, Vol. 2020, No. 5, pp. 1-17, 2020.

[31] Bin Yang, Jinying Zhong, Yuehua Li and Zhongze Chen, "Multi-Focus Image Fusion and Super-Resolution with Convolutional Network", *International Journal of Wavelets, Multiresolution and Information Processing*, Vol. 15, No. 4, pp. 1-15, 2017.